https://doi.org/10.15407/ujpe63.3.204

P.M. TOMCHUK, V.N. STARKOV

Institute of Physics, Nat. Acad. of Sci. of Ukraine, Department of Theoretical Physics
(46, Nauky Ave., Kyiv 03680; e-mail: vjachnikstar@gmail.com)

INFLUENCE OF SHAPE SPREAD IN AN ENSEMBLE OF METAL NANOPARTICLES ON THEIR OPTICAL PROPERTIES

The theoretical basis of the work consists in that the dissipative processes in non-spherical nanoparticles, whose sizes are smaller than the mean free path of electrons, are characterized by a tensor quantity, whose diagonal elements together with the depolarization coefficients determine the half-widths of plasma resonances. Accordingly, the averaged characteristics are obtained for an ensemble of metal nanoparticles with regard for the influence of the nanoparticle shape on the depolarization coefficients and the components of the optical conductivity tensor. Three original variants of the nanoparticle shape distribution function are proposed on the basis of the joint application of the Gauss and "cap" functions.

K e y w o r d s: nanosystem, optics, metal nanoparticles, averaged parameters.

1. Introduction

The optical properties of ensembles of metal nanoparticle are characterized by the presence of plasma resonances in them. The number of these resonances, their frequency positions, and decrements depend on the metal nanoparticle shape (see, e.g., works [1, 2]). It is rather difficult to create an ensemble of absolutely identical nanoparticles. Therefore, while experimentally studying the processes of light absorption and scattering by real ensembles, effective (averaged) optical characteristics are dealt with, as a rule. The procedures of averaging the optical characteristics for an ensemble of spheroidal metal nanoparticles were described, for example, in works [3, 4].

While studying the influence of the shape of metal nanoparticles on their optical properties, the authors of previous papers supposed that dissipative processes in nanoparticles are characterized by a scalar parameter, the high-frequency conductivity. However, we have demonstrated [2, 5, 6] that if the size of non-spherical nanoparticles is smaller than the mean free path of an electron, the optical conductivity is no more a scalar quantity, but acquires a tensor character. The diagonal elements of this tensor together with the depolarization coefficients determine the half-widths of plasma resonances [2, 8]. In this case, averaging over the nanoparticle shapes cannot be reduced to averaging over the depolarization coefficients [3]. Therefore, in this work, theoretical foundations forming the basis for the research of optical properties of an ensemble of elliptic metal nanoparticles, including the components of the optical conductivity tensor, the components of the depolarization tensor, and the absorption coefficient, which were obtained earlier [2, 5, 6, 8], are expounded consistently and in brief. Each stage of research is illustrated by graphic dependences.

The theoretical basis is used to obtain the averaged characteristics for an ensemble of metal nanoparticles with regard for the influence of nanoparticle shapes on the depolarization coefficients and the components of the optical conductivity tensor. The influence of the nanoparticle shape on the conductivity is taken into account in the averaging procedure for the first time.

2. Formulation of the Problem

Let us consider an ensemble of ellipsoidal metal nanoparticles in a dielectric matrix. The nanoparticles are assumed to have the same volume, being some different in shape. Our task consists in elucidating in the framework of this model how the nanoparticle shape spread affects the averaged optical characteristics of the ensemble such as the coefficients of light absorption and scattering. To simplify the model and to obtain a final result, we assume that the nanoparticles are ellipsoids of rotation (spheroids). In this case, the nanoparticle shape can be characterized by a single parameter (the eccentricity or the ratio between the curvature radii). Therefore, the distribution function of nanoparticles over their shape will depend on this parameter only.

Hence, let an ensemble of metal nanoparticles be irradiated with a monochromatic electromagnetic wave. The electric field of the wave looks like

$$\mathbf{E} = \mathbf{E}_0\, e^{i(\mathbf{kr}-\omega\, t)}, \tag{1}$$

where $\mathbf{E}_0$, ω, and $\mathbf{k}$ are the amplitude, frequency, and wave vector, respectively, of the field; and the coordinates and time are denoted by $\mathbf{r}$ and t, respectively. The electromagnetic wave length $\lambda = 2\pi c/\omega$ is assumed to be much larger than the characteristic size of nanoparticles,

$$\lambda \gg \max\{R_i\} \;\; (i = 1, 2, 3), \tag{2}$$

where R_i are the curvature radii. In this case, the electric field induced in an ellipsoidal metal particle by the external wave field (1) is uniform, being connected to the external field $\mathbf{E}_0$ by means of the relation [7, 8]

$$E^i_{\rm in} = \frac{E^j_0}{1 + L_j\,(\epsilon_{jj} - 1)}, \tag{3}$$

where L_j are the principal values of the depolarization tensor components, and ε_{jj} are the diagonal components of the dielectric permittivity tensor. In the case of ellipsoidal metal particles and in the optical spectral interval, the components ε_{jj} can be written in the form [7, 8]

$$\epsilon_{jj} = 1 - \frac{\omega_\rho^2}{\omega^2} + i\frac{4\pi}{\omega}\sigma_{jj}(\omega) \equiv \epsilon' + i\frac{4\pi}{\omega}\sigma_{jj}(\omega), \tag{4}$$

where $\omega_p = (4\pi n_0 e^2/m)^{1/2}$ is the plasma frequency, e the elementary charge, m the electron mass, and n_0 the electron concentration.

In works [2, 5, 6], it was shown that, in the case of a non-spherical nanoparticle, whose dimensions are less than the electron free path, the optical conductivity parameter transforms from the scalar quantity to the tensor one. In the dipole approximation (2), when the internal field $\mathbf{E}_{\rm in}$ in the metal particle is known and looks like Eq. (3), we can determine the influence of this field on the electron distribution function over the velocities. As was shown in works [2, 5, 6], a correction to the equilibrium Fermi distribution function induced by the field $\mathbf{E}_{\rm in}$ has the form

$$f_1\,(\mathbf{r}, \boldsymbol{\vartheta}) = -e\,\mathbf{E}_{\rm in}\boldsymbol{\vartheta}\frac{\partial f_0}{\partial \varepsilon}\left(\frac{1 - e^{-\tilde{\nu}\, t_0}}{\tilde{\nu}}\right), \tag{5}$$

where $\tilde{\nu} = \nu - i\omega$, where ν is the frequency of electron collisions in the nanoparticle bulk, and t_0 is the characteristic of the linearized (in the field) kinetic equation

$$t_0 = \frac{1}{\vartheta'^2}\left\{\mathbf{r}'\vartheta' + \sqrt{(R^2 - r'^2)\vartheta'^2 + \mathbf{r}'\boldsymbol{\vartheta}'}\right\}. \tag{6}$$

Here, $\mathbf{r}'$ and $\boldsymbol{\vartheta}'$ are the coordinate and velocity vectors, respectively, in a deformed coordinate systems, where the ellipsoid has a spherical shape [2, 6]. The relations between the deformed and non-deformed components are very simple:

$$\vartheta'_i = \frac{R_i}{R}\vartheta_i, \quad x'_i = \frac{R_i}{R}x_i, \tag{7}$$

where

$$R = (R_1 R_2 R_3)^{1/3}$$

is the ellipsoid curvature radius.

Expression (5) does not include a contribution of eddy currents to the absorption (magnetic absorption). This mechanism was considered in works [2, 5] in detail, taking the scattering of electrons both in the bulk and at the cluster surface into account. In the visible frequency interval, the contribution of the magnetic absorption is small as compared to the electrical one. Therefore, the former is neglected. More information concerning the magnetic absorption can be found, for example, in work [9].

With the help of the distribution function, we can find the density of the high-frequency current generated by the external field (1) in a nanoparticle:

$$\mathbf{j} = \frac{2e}{(2\pi\hbar)^3}\int \boldsymbol{\vartheta}\, f_1(\mathbf{r},\boldsymbol{\vartheta})\, d^3(m\vartheta). \quad (8)$$

Knowing the current density vector $\mathbf{j}(\mathbf{r},t)$, it is easy to determine the electric dipole moment $\mathbf{d}_0$ of a metal nanoparticle from the relation

$$\frac{\partial}{\partial t}\mathbf{d}_0(t) = \int\limits_V d^3r\, \mathbf{j}(\mathbf{r},t), \quad (9)$$

The optical characteristics of metal nanoparticles and their ensembles, including the corresponding coefficients of light absorption and scattering, can be expressed, in the general case, in terms of the known vectors $\mathbf{j}\,(\mathbf{r},t)$ and $\mathbf{d}_0$. For instance, the coefficient of light absorption by a metal particle with the volume V, which is located in a matrix with the dielectric constant ε_m, equals

$$K\,(\omega) = \\ = \frac{1}{2}\mathrm{Re}\int\limits_V d\mathbf{r}\,(\mathbf{j}\,(\mathbf{r},\omega)\,\mathbf{E}^*_m\,(\mathbf{r},\omega))/\Big(\frac{c}{8\pi}\sqrt{\epsilon_m}|E^{(0)}|^2\Big). \quad (10)$$

If the interaction between the dipoles induced by the wave in different nanoparticles can be neglected (it depends on the nanoparticle concentration), the absorption coefficient for an ensemble of metal nanoparticles is reduced to the sum of absorption contributions from separate particles.

The scattering cross-section can be determined in a similar way. In particular, the average (over the oscillation period) radiation intensity generated by an electric dipole into the solid angle $d\Omega$ at the distance R_0 from the nanoparticle equals [7]

$$dW_s = \frac{c}{8\pi}\,|\,[\mathbf{E}'\times\mathbf{H}']\,|\,R_0^2\,d\Omega = \frac{c}{8\pi}\,|\mathbf{H}'|^2\,R_0^2\,d\Omega. \quad (11)$$

where $\mathbf{E}'$ and $\mathbf{H}'$ are the electric and magnetic components, respectively, of the wave emitted by the dipole ($E' = H'$),

$$\mathbf{H}' = \frac{\omega^2}{c^2 R_0}(\mathbf{n}\times\mathbf{d}_0), \quad (12)$$

and the unit vector $\mathbf{n}$ defines the direction of observation. The ratio between quantity (11) and the irradiation flux intensity determines the scattering cross-section.

Above, we briefly described a procedure of obtaining the optical characteristics for metal nanoparticles and the expressions for the absorption coefficient and the scattering cross-section, proceeding from finding the influence of an electromagnetic wave on the velocity distribution function of electrons. One may get acquainted with the construction of the theory of light absorption and scattering by elliptic metal nanoparticles in works [2, 5, 6, 8] in more details.

3. Optical Parameters of an Ensemble of Elliptic Metal Nanoparticles

Below, an ensemble of spheroidal (ellipsoids of rotation) metal nanoparticles will be considered. This form is the simplest asymmetric one, because its degree of asymmetry is characterized by a single dimensionless parameter, the eccentricity or the ratio between the curvature radii. We are interested first of all in how the dispersion of nanoparticle shapes affects the optical characteristics of the ensemble (recall that the nanoparticle shape governs the number of plasma resonances and their frequencies). In this connection and for simplicity, let us analyze a collection of nanoparticles with the same volume V, but with different eccentricities e_p.

The coefficient of light absorption by a single spheroidal metal nanoparticle can be obtained from Eq. (10) making use of the following expression for the energy absorbed by such nanoparticles [2],

$$K\,(\omega) = \frac{4\pi}{3}V\frac{\epsilon_m^{3/4}}{c}\times \\ \times\Bigg\{\frac{2\sigma_\perp}{\left[\epsilon_m + L_\perp\,(\epsilon' - \epsilon_m)\right]^2 + \left(4\pi\,L_\perp\sigma_\perp/\omega\right)^2} + \\ + \frac{\sigma_\parallel}{\left[\epsilon_m + L_\parallel\,(\epsilon' - \epsilon_m)\right]^2 + \left(4\pi L_\parallel\sigma_\parallel/\omega\right)^2}\Bigg\}, \\ \omega\in[\omega_1,\,\omega_2]. \quad (13)$$

in which the averaging over the orientations of the spheroids' symmetry axes was already carried out. The notations $\sigma_\perp$ and $\sigma_\parallel$ in Eq. (13) are used for the components of the optical conductivity tensor. In the coordinate system where the axis OZ is directed along the symmetry axis of the spheroid, the

diagonal components of the optical conductivity tensor are

$$\sigma_{xx} = \sigma_{yy} \equiv \sigma_{\perp}; \quad \sigma_{zz} \equiv \sigma_{\parallel}. \tag{14}$$

Analogously,

$$L_x = L_y \equiv L_{\perp}; \quad L_z = L_{\parallel}, \tag{15}$$

where the main components of the depolarization tensor equal

$$L_x = L_y = \frac{1}{2}(1 - L_z) \equiv L_{\perp}; \quad L_{\perp} = \frac{1}{2}(1 - L_{\parallel});$$

$$L_z \equiv L_{\parallel} = \begin{cases} \dfrac{1 - e_p^2}{2e_p^3}[\ln\left(\dfrac{1 + e_p}{1 - e_p}\right) - 2e_p], \\ \text{for } R_{\parallel} > R_{\perp}, \\ \dfrac{1 + e_p^2}{e_p^3}(e_p - \arctan e_p), \\ \text{for } R_{\parallel} < R_{\perp}, \end{cases} \tag{16}$$

where $e_p^2 \equiv \left|1 - R_{\perp}^2/R_{\parallel}^2\right|$, and $R_{\perp}$ and $R_{\parallel}$ are the semiaxes of the spheroid.

In works [2, 5], it was shown that, unlike the spherical shape, for a non-spherical metal nanoparticle smaller than the electron free path, the optical conductivity becomes a tensor. In the cited works, the components of this tensor were also studied for ellipsoid-like nanoparticles both in the general case and in various limiting cases.

We are interested in the expressions for non-zero components $\sigma_{\perp}$ and $\sigma_{\parallel}$ of the optical conductivity tensor for spheroidal nanoparticles. The consideration is confined to the case where the influence of the particle shape on the optical conductivity tensor components is maximum. This situation takes place if the surface electron scattering dominates. Expression (5) makes allowance for both the bulk electron scattering (the parameter ν) and the surface electron scattering (the characteristic t_0). Purely surface scattering of electrons is formally obtained by putting $\nu \to 0$, but, actually, the inequality $\nu \ll \upsilon_{\mathrm{F}}/R$ is meant, i.e. the frequency of electron collisions in the bulk is supposed to be small in comparison with the frequency of electron bouncing from wall to wall. For details of the calculation of Eq. (8), see works [2, 5].

As a result, we obtain

$$\sigma_{\perp} = \frac{3\sigma_0}{16} \times$$

$$\times \begin{cases} \dfrac{\left(1 - e_p^2\right)^{1/3}}{e_p^3}\left[e_p\left(1 + 2e_p^2\right) - \left(1 - 4e_p^2\right) \times\right. \\ \left. \times \left(1 - e_p^2\right)^{-1/2} \arcsin e_p\right] \text{ for } R_{\perp} < R_{\parallel}, \\ \dfrac{\left(1 + e_p^2\right)^{1/3}}{e_p^3}\left[-e_p\left(1 - 2e_p^2\right) + \left(1 + 4e_p^2\right) \times\right. \\ \left. \times \left(1 + e_p^2\right)^{-1/2} \ln\left(e_p + \sqrt{1 + e_p^2}\right)\right] \text{ for } R_{\perp} > R_{\parallel}, \end{cases} \tag{17}$$

$$\sigma_{\parallel} = \frac{3\sigma_0}{8} \times$$

$$\times \begin{cases} \dfrac{\left(1 - e_p^2\right)^{1/3}}{e_p^3}\left[-e_p\left(1 - 2e_p^2\right) + \left(1 - e_p^2\right)^{-1/2} \times\right. \\ \left. \times \arcsin e_p\right] \text{ for } R_{\perp} < R_{\parallel}, \\ \dfrac{\left(1 + e_p^2\right)^{1/3}}{e_p^3}\left[e_p\left(1 + 2e_p^2\right) - \left(1 + e_p^2\right)^{-1/2} \times\right. \\ \left. \times \ln\left(e_p + \sqrt{1 + e_p^2}\right)\right] \text{ for } R_{\perp} > R_{\parallel}, \end{cases} \tag{18}$$

where

$$\nu_s = \upsilon_{\mathrm{F}}/2R \tag{19}$$

is the frequency of the electron bouncing from wall to wall in a spherical particle with the volume equal to the volume of ellipsoidal particle, υ the Fermi velocity, and R the radius. In the case of spherical nanoparticles (at $e_p \to 0$), formulas (17) and (18) reproduce the well-known result

$$\sigma_0 = \frac{3n_0e^2}{2m\omega^2}\,\nu_s = \frac{n_0e^2}{m\omega^2}\left(\frac{3}{4}\frac{\upsilon_{\mathrm{F}}}{R}\right). \tag{20}$$

Formulas (17) and (18) do not contain omitted oscillating terms arising due to the resonance between the external electromagnetic wave and electron bouncing frequencies. In the visible spectral interval, this resonance is not actual (for more details, see works [10, 11]).

As one can see from Eqs. (16), (17), and (18), the particle shape governs (through the particle eccentricity) not only the principal values of the depolarization tensor components, but also the principal values of the optical conductivity tensor. Therefore, when averaging over the shape spread, the both dependences have to be taken into account.

As was already said above, expression (13) describes the absorption coefficient for an arbitrary spheroidal metal nanoparticle with the volume V

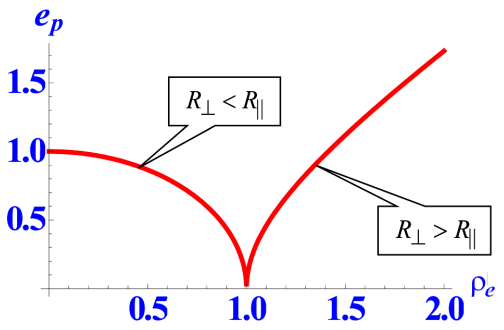

Fig. 1. Dependence of the eccentricity $e_p = \sqrt{|1-\rho_e^2|}$ on the parameter $\rho_e = R_\perp/R_\parallel$

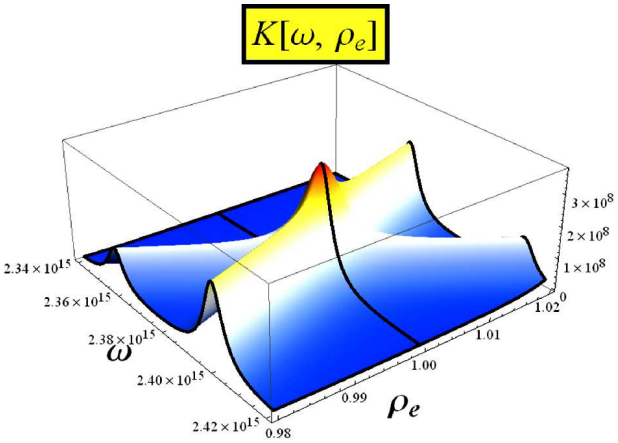

Fig. 2. Dependence $K(\omega, \rho_e)$ of the coefficient of light absorption by a spheroidal metal nanoparticle on its form (the parameter ρ_e) and the light frequency ω

and the parameter e_p (or ρ_e). Expression (13) already takes into account the averaging over the orientations of the spheroid symmetry axis. Figure 1 demonstrates that the relation between the eccentricity $e_p = \sqrt{|1 - R_\perp^2/R_\parallel^2|}$ and the ratio of the curvature radii is ambiguous. Therefore, in what follows, it is more convenient to average the optical characteristics over the parameter $\rho_e = R_\perp/R_\parallel$ and use expression (13) for the coefficient of light absorption by a spheroidal metal nanoparticle in the form

$$K(\omega,\rho_e) = \frac{4\pi\epsilon_m^{3/2}}{3c}\Big\{2\sigma_\perp(\omega,\rho_e)/$$
$$/\left\{\left[\epsilon_m + L_\perp(\rho_e)(\epsilon' - \epsilon_m)\right]^2 + \right.$$
$$+ \left.(4\pi L_\perp(\rho_e)\sigma_\perp(\omega,\rho_e)/\omega)^2\right\} +$$
$$+ \sigma_\parallel(\omega,\rho_e)/\left\{\left[\epsilon_m + L_\parallel(\rho_e)(\epsilon' - \epsilon_m)\right]^2 + \right.$$
$$+ \left.\left(4\pi L_\parallel(\rho_e)\sigma_\parallel(\omega,\rho_e)/\omega\right)^2\right\}\Big\},$$
$$\omega \in [\omega_1\omega_2],\ \rho_e \in [0,\infty). \qquad (21)$$

In Fig. 2, the dependence of the light absorption coefficient K on the particle shape (the parameter ρ_e) and the light frequency ω is shown. Two ridges on the surface correspond to two plasma resonances. At $\rho_e = 1$, those ridges intersect each other, which corresponds to the plasma resonance in a spherical nanoparticle.

Let the distribution function of metal nanoparticles over their shapes look like

$$\Phi(\rho_e) = NP(\rho_e).$$

Here, N is the nanoparticle concentration, and the quantity $P(\rho_e)$ is the probability that an ensemble of N nanoparticles contains a nanoparticle, whose form is characterized by the parameter ρ_e (below, the subscript e is omitted). This probability is normalized to unity, so that

$$\int_0^\infty P(\rho)\,d\rho = 1.$$

In this case, the effective value of the total absorption coefficient equals

$$\overline{K(\omega)} = \int_0^\infty K(\omega,\rho)\,P(\rho)\,d\rho. \qquad (22)$$

4. Selection of Expression for the Function $P(\rho)$

The function $P(\rho)$, which describes the probability to find a nanoparticle with a given ρ-value ($\rho \in [0,\infty)$) in a unit volume, can be interpreted as the probability density for the function $K(\omega,\rho)$, and the function $\overline{K(\omega)}$ as the shape-averaged coefficient of total absorption for the ensemble of nanoparticles.

As a first step to construct $P(\rho)$, let us consider the normal (Gauss) distribution law, which is widely applied when solving practical problems. According to this law, the probability density for a normally distributed random variable is expressed by the formula

$$P_g(x) = \frac{1}{\sigma_g\sqrt{2\,\pi}}\exp\left(-\frac{(x-a_g)^2}{2\,\sigma_g^2}\right), \qquad (23)$$
$$x \in (-\infty,+\infty),$$

where a_g and σ_g are the mathematical expectation and the mean square deviation, respectively, of the random variable. It is important to emphasize that the support of the Gauss function (23) includes the entire number axis, i.e. $x \in (-\infty, +\infty)$. At the same time, the support of the sought function $P(\rho)$ is the non-negative semiaxis, $\rho \in [0, \infty)$. Therefore, in order to adequately make allowance for the presence of oblate nanoparticles with $R_\perp \geq R_\parallel \to 0$ in the ensemble, the application of the Gauss function

$$P_1(\rho) = \alpha_1 \exp[-\beta_1(\rho - a)^2], \ \rho \in (a, \infty), \ a \geq 0 \quad (24)$$

in the interval $\rho \in (a, \infty)$ is justified.

A second step to construct the function $P(\rho)$ consists in selecting an expression $P_0(\rho)$ with the support $\rho \in [0, a]$, in which the main contribution to the averaging of $K(\omega, \rho)$ is provided by prolate nanoparticles with $R_\parallel \geq R_\perp \to 0$. In particular, the expression for $P_0(\rho)$ should satisfy three general requirements:

1. $P_0(\rho)$ must be continuous at the point $\rho = a$, i.e. $P_0(a) = P_1(a)$;

2. $P_0(\rho)$ must be sufficiently smooth, i.e. $P_0(\rho) \in \in C^{(m)}(0, a)$, where $m \geq 2$, since the Gauss function is infinitely differentiable;

3. the condition $P_0(0) = 0$ must be obeyed by analogy with $P_1(\rho)$, when $\lim_{\rho \to \infty} P_1(\rho) = 0$.

Those requirements are satisfied by the "cap" function [13]

$$P_\gamma(x) = \begin{cases} C_\gamma \exp[-\gamma^2/(\gamma^2 - x^2)], & |x| < \gamma, \\ 0, & |x| \geq \gamma, \end{cases} \quad (25)$$

where the constant C_γ is chosen so that $\int \omega_\gamma(x)dx = = 1$, i.e.

$$C_\gamma = \left(2\gamma \int\limits_0^1 \exp\left[-(1 - \xi^2)^{-1}\right] d\xi \right)^{-1}.$$

This function is infinitely differentiable ($P_\gamma(x) \in \in C^{(\infty)}(-\gamma, \gamma)$). However, unlike the Gauss function, its support is finite, $\operatorname{supp} P_\gamma(x) = (-\gamma, \gamma)$, i.e. the function is compact. These properties make the function $P_\gamma(x)$ very attractive, while solving a large number of specific problems [14].

As an example of the joint application of the Gauss [Eq. (24)] and "cap" [Eq. (25)] functions, let us construct the function (see Fig. 3)

$$P_1(\rho) = P_{0\mathrm{I}}(\rho) + P_{1\mathrm{I}}(\rho), \quad (26)$$

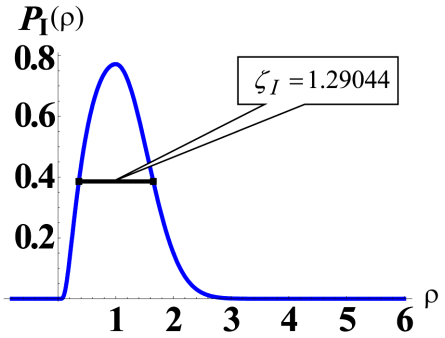

Fig. 3. An example of the function $P_1(\rho)$ as a combination of the cap function (27) in the interval $\rho = [0, 1]$ and the Gauss function (28) in the interval $\rho = (1, +\infty)$. The half-width of the function $\zeta_\mathrm{I} = 1.29044$

where

$$P_{0\mathrm{I}}(\rho) = = \begin{cases} 0.771606 \exp[-(\rho-1)^2/(1-(\rho-1)^2)], & \rho \in [0, 1], \\ 0, & \rho \notin [0, 1], \end{cases} \quad (27)$$

$$P_{1\mathrm{I}}(\rho) = = \begin{cases} 0.771606 \exp[-1{,}63754(\rho-1)^2], & \rho \in (1, +\infty), \\ 0, & \rho \in (-\infty, 1]. \end{cases} \quad (28)$$

Note that the expression proposed for the function $P(\rho)$ is based on the heuristic principle. The application of the latter significantly simplifies the solution of a rather complicated problem concerning the influence of the metal nanoparticle shape dispersion on the total absorption coefficient.

Surely, the heuristic approach does not guarantee that the selected expression for the function $P(\rho)$ is optimal. Moreover, in effect, this trick does not guarantee at all that the expected result will quantitatively coincide with the experiment. Nevertheless, we may assert *a priori* that the worth of the joint application of the Gauss [Eq. (24)] and "cap" [Eq. (25)] functions consists in that a solution was proposed, which turns out to be optimal for a theoretical study of the qualitative picture obtained, when averaging over the nanoparticle shape spread. As an argument in favor of the selected variant, it can be the histograms of nanoparticle size distribution [15].

A necessary requirement for obtaining adequate quantitative results for the problem under consideration is the presence of experimentally measured

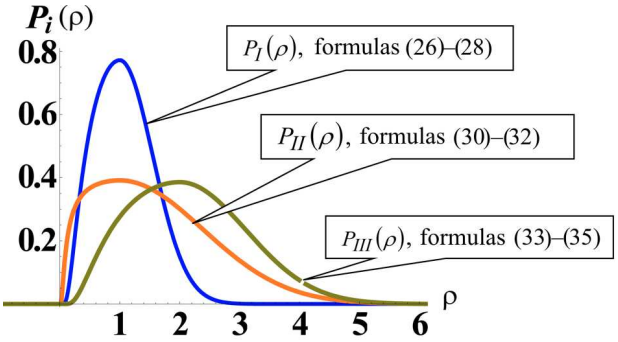

Fig. 4. Probability functions $P_i\,(\rho)$ describing the presence of nanoparticles with definite shapes in the ensemble

data for the effective value of the total absorption coefficient $\overline{K\,(\omega)}$. The knowledge of this value makes it possible to interpret relation (22) written in the form

$$\int\limits_0^\infty K\,(\omega,\rho)\,P\,(\rho)\,d\rho = \overline{K\,(\omega)}$$

as an integral Fredholm equation of the first kind, in which the functions $K\,(\omega,\rho)$ and $\overline{K\,(\omega)}$ are known, whereas the function $P\,(\rho)$ is to be determined. The solution of the Fredholm equation of the first kind is a rather complicated task, because this is an ill-posed (in the Hadamard sense) problem [12]. Briefly speaking, the problem is well-posed if it has a solution, and this solution is unique and continuously depends on the input data. If one of those conditions is not satisfied, the peoblem is ill-posed or, simply, incorrect.

One should bear in mind that, for a well-posed problem, small errors in the initial data are not crucial, because their impact on the solution is insignificant. A completely different situation arises if there are small errors in the input data for an ill-posed problem, because its solution is very sensitive to errors. In the case of optical experimental researches, it is the third condition that most often is not satisfied. Its analysis brings us to the following conclusion: Insignificant changes in the input data for $K\,(\omega,\rho)$ or $\overline{K\,(\omega)}$ may result in arbitrarily large changes in the output data for $P\,(\rho)$. The main method to study the integral equation of the first kind is the regularization one. A detailed example of its implementation was considered in work [14].

5. Results of Computational Experiment and Their Interpretation

In the corresponding computational experiments, the following parameter values were used as input ones:

$$\omega_p = 1.37\times10^{16}\ \mathrm{s}^{-1};\quad \upsilon = 3.39\times10^{13}\ \mathrm{s}^{-1};$$
$$R = 2.0\times10^{-6}\ \mathrm{cm};\quad c = 3.0\times10^{10}\ \mathrm{cm\cdot s}^{-1};$$
$$v_{\mathrm{F}} = 1.39\times10^{8}\ \mathrm{cm\cdot s}^{-1};\quad n = 10^{22};$$
$$m = 10^{-27}\ \mathrm{g};\quad \epsilon_m = 16.$$

As a first result of computations, the three-dimensional representation of the dependence $K(\omega,\rho)$ for the absorption coefficient of a spheroidal metal nanoparticle with an arbitrary shape in the intervals $\omega \in [8\times10^{14},\ 8\times10^{15}]$ and $\rho \in [0, 10]$ should be exhibited. A fragment of this dependence in a vicinity of the spherical nanoparticle is shown in Fig. 2. Preliminarily, we obtained computational formulas for calculating the components $\sigma_\perp(\omega,\ \rho)$ and $\sigma_\parallel(\omega,\ \rho)$ of the optical conductivity tensor for a spheroidal shape and the principal values for the depolarization tensor components $L_\perp$ and $L_\parallel$.

The main result of the computational experiment includes the effective values for the total absorption coefficients

$$\overline{K_i\,(\omega)} = \int\limits_0^\infty K\,(\omega,\rho)\,P_i\,(\rho)\,d\rho \tag{29}$$

found for various functions $P_i(\rho)$, i = I, II, III. The latter evaluate the probability for the nanoparticles with a specific shape to exist in the ensemble. The plots of the functions $P_i(\rho)$ are depicted in Fig. 4, and the specific expressions for the functions $P_{\mathrm{II}}(\rho)$ and $P_{\mathrm{III}}(\rho)$ are as follows:

$$P_{\mathrm{II}}(\rho) = P_{0\mathrm{II}}(\rho) + P_{1\mathrm{II}}(\rho), \tag{30}$$

$$P_{0\mathrm{II}}(\rho) =$$

$$= \begin{cases} 0.391277\exp\left\{-0.097151[1+(\rho-1)^2]/\right. \\ \left./[1-(\rho-1)^2]\right\},\ \rho\in(0,\ 1], \\ 0,\ \rho\notin(0,\ 1], \end{cases} \tag{31}$$

$$P_{1\mathrm{II}}(\rho) =$$

$$= \begin{cases} 0.391277\exp[-1.63754(\rho-1)^2],\ \rho\in(1,+\infty), \\ 0,\ \rho\in(-\infty,\ 1]. \end{cases} \tag{32}$$

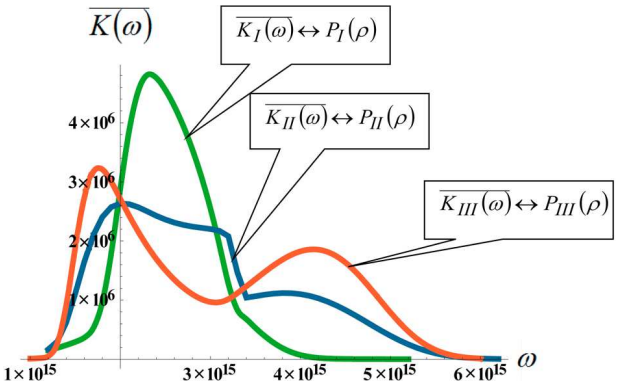

Fig. 5. Averaged coefficientsof total absorption $\overline{K_i(\omega)}$, i = I, II, III, normalized to the nanoparticle concentration N

$$P_{\rm II}(\rho) = P_{0\rm III}(\rho) + P_{1\rm III}(\rho), \tag{33}$$

$$P_{0\rm III}(\rho) = $$

$$= \begin{cases} 0.385803\exp[-(\rho-2)^2/(4-(\rho-2)^2)], & \rho\in[0,\,2], \\ 0, & \rho\notin(0,\,2], \end{cases} \tag{34}$$

$$P_{1\rm III}(\rho) = $$

$$= \begin{cases} 0.385803\exp[-0.409384(\rho-2)^2], & \rho\in(2,+\infty), \\ 0, & \rho\in(-\infty,\,2]. \end{cases} \tag{35}$$

Figure 5 demonstrates plots for the effective values of the total absorption coefficients $\overline{K_i(\omega)}$, i = I, II, III, which, according to Eq. (29), correlate with the values of the functions $P_i(\rho)$.

The nanoparticle shape is responsible for both the principal values of the depolarization tensor components $L_\perp$ and $L_\parallel$, and the principal values of the optical conductivity tensor $\sigma_\perp$ and $\sigma_\parallel$. Therefore, when averaging the absorption coefficient $K(\omega,\rho)$ over the nanoparticle shape spread, the visualization of the dependences $\widehat{\sigma}_\perp(\rho) = \sigma_\perp(\omega_0,\rho)/\sigma_0(\omega_0)$ and $\widehat{\sigma}_\parallel(\rho) = \sigma_\parallel(\omega_0,\rho)/\sigma_0(\omega_0)$, in our opinion, is reasonable (Fig. 6).

After having compared the dependence of the coefficient of light absorption by a spheroidal metal nanoparticle on its shape (the parameter ρ_e) and the light frequency ω shown in Fig. 2 with the plots for the average total absorption coefficients $\overline{K_i(\omega)}$ depicted in Fig. 5, we arrive at a conclusion that those values differ by about two orders of magnitude. Nevertheless, the discussed dependences are characterized by some general features. For our conclusions to be more specific, let us consider the plots of the functions $\overline{K_i(\omega)}$

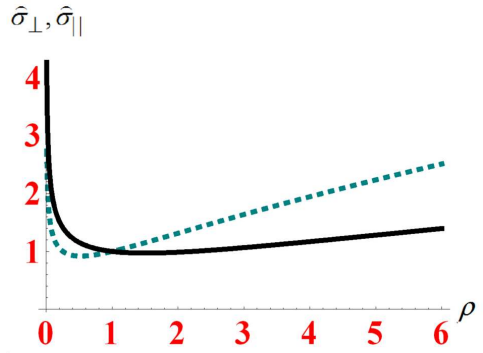

Fig. 6. Transverse (solid curve) and longitudinal (dashed curve) components of the optical conductivity tensor

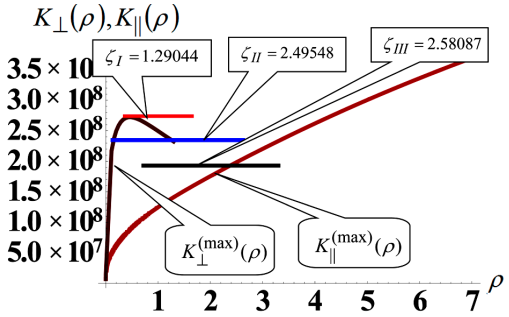

Fig. 7. Projections of the maximum values of the orthogonal, $K_\perp^{(\max)}(\rho)$, and parallel, $K_\parallel^{(\max)}(\rho)$, components of the coefficient $K(\omega,\rho)$ of light absorption by a spheroidal metal nanoparticle on the plane (K,ρ), and the half-widths of the functions $P_i(\rho)$, i = I, II, III

(Fig. 5) in more details. There arises a simple question: Why do the plots have the exhibited dependence on the light frequency ω? To answer it, let us introduce two functions, $K_\perp^{(\max)}(\rho)$ and $K_\parallel^{(\max)}(\rho)$, into consideration. They correspond to the first and second, respectively, summands in Eq. (21), being the projections of the maximum values of the orthogonal and parallel, respectively, components of the light absorption coefficient $K(\omega,\rho)$ by a spheroidal metal nanoparticle onto the plane (K,ρ) (see Fig. 7). In other words, $K_\perp^{(\max)}(\rho)$ and $K_\parallel^{(\max)}(\rho)$ are the projections of the surface ridges corresponding to two plasma resonances (Fig. 2) onto the plane (K,ρ).

They are described by the expressions

$$K_{\perp,\parallel}^{(\max)}(\rho) = $$

$$= \frac{\chi_{\perp,\parallel}\,\omega_p^2}{[\epsilon_m + L_{\perp,\parallel}(\rho)\,(1-\epsilon_m)]\,L_{\perp,\parallel}(\rho)\,\sigma_{\perp,\parallel}(\omega_{\perp,\parallel},\rho)}, \tag{36}$$

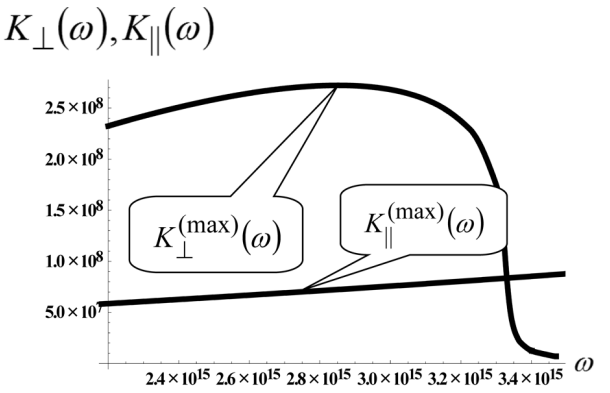

Fig. 8. Projections of the maximum values of the orthogonal, $K_\perp^{(\max)}(\omega)$, and parallel, $K_\parallel^{(\max)}(\omega)$, components of the coefficient $K(\omega,\rho)$ of light absorption by a spheroidal metal nanoparticle on the plane (K,ω) in the interval $\omega \in (2.2\times10^{15}\ \mathrm{s}^{-1}, 3.47\times10^{15}\ \mathrm{s}^{-1})$

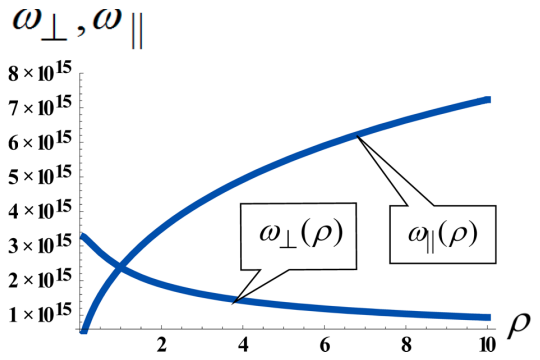

Fig. 9. Dependences of the orthogonal, $\omega_\perp$, and parallel, $\omega_\parallel$, resonance frequencies on the parameter ρ

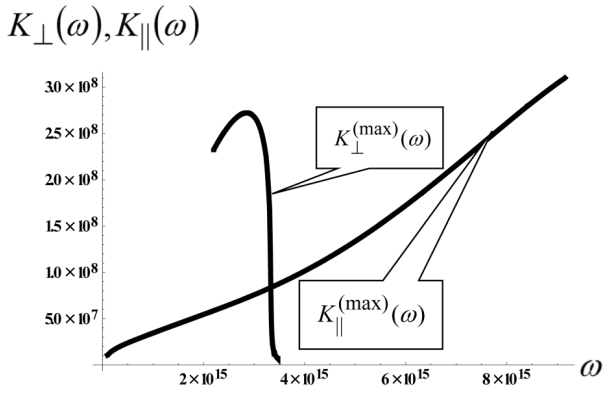

Fig. 10. Projections of the maximum values of the orthogonal, $K_\perp^{(\max)}(\omega)$, and parallel, $K_\parallel^{(\max)}(\omega)$, components of the coefficient $K(\omega,\rho)$ of light absorption by a spheroidal metal nanoparticle on the plane (K,ω) in the interval $\omega \in (10^{14}\ \mathrm{s}^{-1}, 9.2\times10^{15}\ \mathrm{s}^{-1})$

where

$$\chi_\parallel = \frac{\epsilon_m^{3/2}}{12\pi\, c}, \quad \chi_\perp = 2\,\chi_\parallel,$$

and

$$\omega_{\perp,\parallel}^2(\rho) = \frac{L_{\perp,\parallel}(\rho)\omega_p^2}{\epsilon_m + L_{\perp,\parallel}(\rho)\,(1-\epsilon_m)}$$

are the frequencies of plasma resonances [1]. Formulas (36) are a rather simple consequence of the modified representation (21) for the coefficient $K(\omega,\rho)$, i.e.

$$K(\omega,\rho) \equiv K_\perp(\omega,\rho) + K_\parallel(\omega,\rho),$$

$$K_\perp(\omega,\rho) = \frac{4\pi\,\epsilon_m^{3/2}}{3c} \times$$

$$\times \frac{2\,\omega^4\sigma_\perp(\omega,\rho)\,/g_\perp^2(\rho)}{(\omega^2-\omega_\perp^2)^2 + [4\pi\,L_\perp(\rho)\sigma_\perp(\omega,\rho)/g_\perp(\rho)]^2\omega^2},$$

$$K_\parallel(\omega,\rho) = \frac{4\pi\,\epsilon_m^{3/2}}{3c} \times$$

$$\times \frac{\omega^4\sigma_\parallel(\omega,\rho)\,/g_\parallel^2(\rho)}{(\omega^2-\omega_\parallel^2)^2 + [4\pi\,L_\parallel(\rho)\,\sigma_\parallel(\omega,\rho)/g_\parallel(\rho)]^2\omega^2},$$

$$g_{\perp,\parallel}(\rho) \equiv \epsilon_m + L_{\perp,\parallel}(\rho)\,(1-\epsilon_m),$$

$$K_{\perp,\parallel}^{(\max)}(\rho) = K_{\perp,\parallel}(\omega_{\perp,\parallel}(\rho),\rho).$$

Three segments in Fig. 7 demonstrate the half-widths of the functions $P_i(\rho)$. The abscissa coordinates of the segment ends accurately correspond to the calculated values

$$\rho_a^{(\zeta_\mathrm{I})} = 0.360169; \quad \rho_b^{(\zeta_\mathrm{I})} = 1.65060;$$
$$\rho_a^{(\zeta_\mathrm{II})} = 0.131587; \quad \rho_b^{(\zeta_\mathrm{II})} = 2.62707;$$
$$\rho_a^{(\zeta_\mathrm{III})} = 0.720338; \quad \rho_b^{(\zeta_\mathrm{III})} = 3.301210.$$

Here, $\rho_a^{(\zeta_i)}$ and $\rho_b^{(\zeta_i)}$ are the initial and final points of the segments ζ_i (i = I, II, III). The ordinates of the segments were selected arbitrarily to make the analysis of the results obtained more convenient. The first thing drawing attention in Figs. 7, 8, and 10 is a small support of the orthogonal component (the ridge) of the light absorption coefficient $K_\perp(\omega,\rho)$. Really, as follows from our calculations, the function $K_\perp^{(\max)}(\rho)$ is determined in the interval $\rho \in (0, 1.414)$ (Fig. 7), whereas the support of the function $K_\perp^{(\max)}(\omega)$ is the interval $\omega \in (2.138\times\times10^{15}\ \mathrm{s}^{-1}, 3.47\times10^{15}\ \mathrm{s}^{-1})$ (see Figs. 8 and 10). On

the other hand, calculations by the expression describing the dependence of the plasma resonance frequencies on the nanoparticle shape demonstrate that the intervalof transverse resonance frequency $\omega_\perp(\rho)$ is confined by the values $\omega_\perp(0) = 3.3227 \times 10^{15}$ s^{-1} and $\omega_\perp(1.41401) = 2.138 \times 10^{15}$ s^{-1} (Fig. 9). Conditionally, we call plasma oscillations in the direction perpendicular to the spheroid axis and, accordingly, to longitudinal oscillations, as "transverse" resonances. Thus, the support of the function $K_\perp^{(\max)}(\omega)$ consists of two sections: the resonance section, $\omega_r \in \in (2.138 \times 10^{15}$ s^{-1}, 3.3227×10^{15} s$^{-1})$, and the deflation [1] section, $\omega_d \in (3.3227 \times 10^{15}$ s$^{-1}, 3.47 \times \times 10^{15}$ s$^{-1})$, in which a sharp recession of $K_\perp^{(\max)}(\omega)$ to background $K(\omega, \rho)$-values takes place. Another important point consists in that there is one plasma resonance in $K_\parallel(\omega, \rho)$ at $\omega > 3.47 \times 10^{15}$ s^{-1}.

By comparing the relative arrangement of the plots of the functions $K_\perp^{(\max)}(\rho)$ and $K_\parallel^{(\max)}(\rho)$ with the half-widths ζ_i of the functions $P_i(\rho)$, $i =$ I, II, III, we arrive at the following conclusions.

• The main factor affecting the function $P_{\rm I}(\rho)$ is the orthogonal component of the coefficient $K(\omega, \rho)$ of light absorption by a spheroidal metal nanoparticle (see $K_\perp^{(\max)}(\rho)$ and $\zeta_{\rm I}$ in Fig. 7). Therefore, tentatively speaking, the curve $\overline{K_{\rm I}(\omega)}$ in the resonance ω_r-interval (Fig. 5) is similar to its prototype $P_{\rm I}(\rho)$ at $\rho < 1.414$. A noticeable change in the character of the $\overline{K_{\rm I}(\omega)}$-curve (Fig. 5) is observed in the deflation ω_d-interval.

• When the function $P_{\rm II}(\rho)$ is mapped by the operator K, the amplitude value $\overline{K_{\rm II}(2.0 \times 10^{15})}$ decreases together with the amplitude of $P_{\rm II}(1.0)$. A substantial change in the $\overline{K_{\rm II}(\omega)}$-plot is observed in the deflation section ω_d and in its right-hand side vicinity, where the influence of $K_\parallel^{(\max)}(\rho)$ (at $\rho > 1.414$) and $K_\parallel^{\max}(\omega)$ (at $\omega > 3.47 \times 10^{15}$ s^{-1}) is appreciable.

• The function $\overline{K_{\rm III}(\omega)}$ obtained for the average value of the total absorption coefficient is the most adequate for a real situation. It completely describes the influence of both the transversal, $K_\perp(\omega, \rho)$, and longitudinal, $K_\parallel(\omega, \rho)$, components of the light absorption coefficient on $P_{\rm III}(\rho)$.

[1] *Deflation* (from the Latin *deflatio*): in geology, this is a process of erosion and removal of loose rock particles by the wind. Small particles of clay, silt, and sand sizes are susceptible to deflation.

6. Conclusions

To summarize, the results of theoretical research concerning the optical characteristics of an ensemble of spheroidal metal nanoparticle – these are the components $\sigma_\perp$ and $\sigma_\parallel$ of the optical conductivity tensor, the principal values of the depolarization tensor components $L_\perp$ and $L_\parallel$, and the absorption coefficient – have been presented. The averaged characteristics were obtained, by considering the influence of the nanoparticle shape on both the depolarization coefficients and the optical conductivity tensor components. While performing the averaging procedure, the influence of the nanoparticle shape on the conductivity is taken into consideration for the first time.

The results of computational experiments are also presented. Specific valueswere used as input data. Recall that the number of plasma resonances, as well as their frequencies and decrements, depends on the nanoparticle shape. In particular, there is a single plasma resonance in the case of spherical particles, two in the case of spheroids, and three for elliptical particles. The result of our calculations inserted a correction: in the case of spheroidal nanoparticles, there are two plasma resonances in the finite frequency interval ($\omega \in (2.138 \times 10^{15}$ s^{-1}, 3.47×10^{15} s$^{-1})$, Fig. 10). Beyond this interval, only one plasma resonance in $K_\parallel(\omega, \rho)$ takes place.

Three variants are proposed for the functions $P_i(\rho)$, $i =$ I, II, III, which describe the distribution of nanoparticles over their shapes. Note that the proposed variant of the expression for the function $P_i(\rho)$ is based on the joint application of the Gauss and "cap" functions, which significantly simplifies the solution of rather a complicated problem concerning the influence of the shape spread in an ensemble of metal nanoparticles on the total absorption coefficient. We may assert that, additionally, the joint application of the Gauss and "cap" functions turns out to be optimal, when theoretically studying the qualitative picture of averaging over the shape spread.

The averaged values of the total absorption coefficients $\overline{K_i(\omega)}$, $i =$ I, II, III, are determined for each variant of the function $P_i(\rho)$ (Fig. 5). The function $\overline{K_{\rm III}(\omega)}$ calculated for the average value of the total absorption coefficient is found to be the most adequate to the real situation. It completely describes the influence of both the transverse, $K_\perp(\omega, \rho)$, and longitudinal, $K_\parallel(\omega, \rho)$, components of the light absorption coefficient on $P_{\rm III}(\rho)$.

1. V.V. Klimov. *Nanoplasmonics* (Fizmatlit, 2012) (in Russian) [ISBN: 978-5-9221-1205-5].
2. P.M. Tomchuk, N.I. Grigorchuk. Shape and size effects on the energy absorption by small metallic particles. *Phys. Rev. B* **73**, 155423 (2006).
3. E.F. Venger, A.V. Goncharenko, M.L. Dmitruk, *Optics of Small Particles and Disperse Media* (Naukova Dumka, 1999) (in Ukrainian).
4. A.V. Goncharenko, E.F.Venger, S.N. Zavadskii. Effective absorption cross section of an assembly of small ellipsoidal particles. *J. Opt. Soc. Am. B* **13**, 2392 (1996).
5. P.M. Tomchuk, B.P. Tomchuk. Optical absorption of small metal particles. *Zh. Eksp. Teor. Fiz.* **112**, 661 (1997) (in Russian).
6. R.D. Fedorovich, A.G. Naumovets, P.M. Tomchuk. Electron and light emission from island metal films and generation of hot electrons in nanoparticles. *Phys. Rep.* **328**, 73 (2000).
7. L.D. Landau, E.M. Lifshits, *Electrodynamics of Continuous Media* (Pergamon Press, 1984).
8. D.V. Butenko, P.M. Tomchuk. The nanoparticle shape's effect on the light scattering cross-section. *Surf. Sci.* **606**, 1892 (2012).
9. S. Tretyakov. *Nanostructured Metamaterials, European Commission*. Edited by S. Tretyakov, P. Barois, T. Scharf *et al.* (Office of the European Union, 2010).
10. N.I. Grigorchuk, P.M. Tomchuk. Cross-sections of electric and magnetic light absorption by spherical metallic nanoparticles. The exact kinetic solution. *Ukr. Fiz. Zh.* **51**, 921 (2006).
11. P.M. Tomchuk, D.V. Butenko. Dependences of dipole plasmon resonance damping constants on the shape of metallic nanoparticles. *Ukr. J. Phys.* **60**, 1042 (2015).
12. V.N. Starkov, *Constructive Methods of Computational Physics in Interpretation Problems* (Naukova Dumka, 2002) (in Russian).
13. V.S. Vladimirov. *Equations of Mathematical Physics* (M. Dekker, 1971).
14. V.N. Starkov, M.S. Brodyn, P.M. Tomchuk, V.Ya. Gayvoronsky, A.Yu. Boyarchuk. Mathematical interpretation of experimental research results on nonlinear optical material properties. *Ukr. J. Phys.* **60**, 601 (2015).
15. W. Haiss, N.T.K. Thanh, J. Aveyard, D.G. Fernig. Determination of size and concentration of gold nanoparticles from UV-vis spectra. *Anal. Chem.* **79**, 4215 (2007).

Received 15.11.18.
Translated from Ukrainian by O.I. Voitenko

П.М. Томчук, В.М. Старков

ВПЛИВ ДИСПЕРСІЇ ФОРМ
АНСАМБЛЮ МЕТАЛЕВИХ НАНОЧАСТИНОК
НА ЇХ ОПТИЧНІ ВЛАСТИВОСТІ

Р е з ю м е

Теоретичну основу роботи становить положення, що при розмірах наночастинок, менших за довжину вільного пробігу електрона і несферичній їх форми, дисипативні процеси всередині наночастинок характеризуються тензорною величиною. Діагональні елементи цього тензора разом з коефіцієнтами деполяризації визначають півширини плазмових резонансів. На основі цього отримані усереднені характеристики з урахуванням впливу форми наночастинок як на коефіцієнти деполяризації, так і на компоненти тензора оптичної провідності. Запропоновано три оригінальних варіанти функцій, побудованих на основі спільного використання функцій Гауса і "шапочки", які задають розподіл наночастинок за формою.